 CMES, vol.76, no.1, pp.61-82, 2011

Iterative Analysis of Pore-Dynamic Models Discretized by Meshless Local Petrov-Galerkin Formulations

Delfim Soares Jr.[1]

Abstract: This work proposes an iterative procedure to analyse pore-dynamic models discretized by time-domain Meshless Local Petrov-Galerkin formulations. By considering an iterative procedure based on a successive renew of variables, each phase of the coupled problem in focus can be treated separately, uncoupling the governing equations of the model. Thus, smaller and better conditioned systems of equations are obtained, rendering a more attractive methodology. A relaxation parameter is introduced here in order to improve the efficiency of the iterative procedure and an expression to compute optimal values for the relaxation parameter is discussed. Linear and nonlinear models are focused, highlighting that the analysis of the nonlinear relations can be carried out along the iterative steps of the coupled model solution, adding no further computational costs to the analysis. At the end of the paper, numerical examples illustrate the performance and potentialities of the proposed techniques.

Keywords: Iterative Analysis; Pore-Dynamics; Optimal Relaxation Parameters; Meshless Local Petrov-Galerkin; Nonlinear Analysis.

1 Introduction

For many everyday engineering problems, such as earthquake engineering, soil-structure interaction, biomechanics, seismic wave scattering etc., dynamic porous media analysis is necessary and over simplified theoretical models may only represent a very crude approximation. Nowadays, several numerical approaches, especially those considering finite element procedures, are available to analyse complex dynamic porous media (see, for instance, Ehlers and Bluhm, 1998; Lewis and Schrefler, 1998; Zienkiewicz *et al.*, 1999; etc.) and most of these approaches are based on the pioneering work of Biot (Biot, 1941; 1956a-b; 1962 – for a complete overview of the porous media theory evolution, the book of de Boer, 1998, is

[1] Structural Engineering Department, Federal University of Juiz de Fora, Cidade Universitária, CEP 36036-330, Juiz de Fora, MG, Brazil. Tel: +55 32 2102-3468; E-mail: delfim.soares@ufjf.edu.br

recommended).

In spite of the great success of the finite element method and other techniques as effective numerical tools for the solution of boundary value problems on complex domains, there is still a growing interest in development of new advanced methods. Nowadays, many meshless formulations are becoming popular, due to their high adaptivity and to their low-cost effort to prepare input data (meshless methods were essentially stimulated by difficulties related to mesh generation). In addition, the need for flexibility in the selection of approximating functions (*e.g.*, the flexibility to use non-polynomial approximating functions) has played a significant role in the development of meshless methods. Many meshless approximations give continuous variation of the first or higher order derivatives of a primitive function in counterpart to classical polynomial approximation, where secondary fields have a jump on the interface of elements; therefore, meshless approximations are leading to more accurate results in many cases.

A variety of meshless methods has been proposed along the last decades (e.g., Belytschko *et al*., 1994; Atluri and Shen, 2002 etc.). Many of them are derived from a weak-form formulation on global domain (Belytschko *et al*., 1994) or a set of local subdomains (Atluri and Zhu, 1998; Atluri and Shen 2002; Mikhailov, 2002; Sladek *et al*. 2003, 2008). In the global formulation, background cells are required for the integration of the weak form. In methods based on local weak formulation, no cells are required (if, for the geometry of the subdomains, a simple form is chosen, numerical integrations can be easily carried out over them) and therefore they are often referred to as truly meshless methods. The Meshless Local Petrov-Galerkin (MLPG) method is a fundamental base for the derivation of many meshless formulations, since trial and test functions are chosen from different functional spaces.

Meshless methods, based on the MLPG approach, were developed and implemented for the solution of the Biot's consolidation problem by Ferronato *et al*. (2007) and Bergamaschi (2009), taking into account axi-symmetric poroelastic models, and by Wang *et al*. (2009), taking into account plane models. The pore-dynamic analysis of elastic soils considering the MLPG was introduced by Soares (2010a), taking into account Gaussian weight functions as test functions and different discretizations for each phase of the model. Later on, Soares (2010b) extended the formulation to consider the dynamic analysis of elastoplastic porous media taking into account MLPG formulations based on Heaviside step functions as test functions.

In the present work, iterative analysis of pore-dynamic models discretized by MLPG procedures is focused. In the Finite Element Method, the iterative analysis of pore-dynamic models does not exhibit convergence unless some especial procedures are considered (see, for instance, Li *et al*., 2003, and Markert *et al*., 2010). In the

Boundary Element Method as well, convergence is hardly achieved considering iterative analysis when pore-dynamic models are focused (Soares *et al*., 2006), although this seems to be an appropriate procedure once static models are considered (Cavalcanti and Telles, 2003). For the MLPG method, on the other hand, as it is described along the present work, iterative analyses are very effective, and convergence can be achieved considering few iterative steps.

This paper is organized as follows: first, the governing equations of the pore-dynamic model are presented (section 2) and, in the sequence, their numerical discretization by MLPG techniques is briefly described (section 3); in section 4, the iterative analysis of the pore-dynamic model is discussed and the evaluation of optimal relaxation parameters is introduced, in order to speed up the convergence of the iterative procedure; finally, in section 5, numerical applications are presented, illustrating the performance and potentialities of the proposed techniques.

2 Governing equations

For a unit volume and from the definition of the total stress, the total momentum equilibrium equation for the solid-fluid ensemble can be written as (Zienkiewicz et al., 1990)

$$\sigma_{ij,j} - \rho_m \ddot{u}_i + \rho_m b_i = \rho_f \left(\dot{w}_i + w_j w_{i,j}\right) \tag{1}$$

where σ_{ij} is the total Cauchy stress, using the usual indicial notation for Cartesian axes; the effective stress is defined as $\sigma'_{ij} = \sigma_{ij} + \alpha\delta_{ij}p$, in which α is the so-called Biot's parameter, accounting for slight strain changes, and p is the pore pressure. In addition, u_i stands for the solid matrix displacement, w_i for the mean fluid velocity relative to the solid phase and b_i for the body force distribution. Inferior commas and overdots indicate partial space ($u_{j,i} = \partial u_j/\partial x_i$) and time ($\dot{u}_i = \partial u_i/\partial t$) derivatives, respectively. The density of the mixture is defined as $\rho_m = \mu\rho_f + (1-\mu)\rho_s$, where ρ_s and ρ_f are the density of the solid and fluid phase, respectively, and μ is the porosity of the solid.

The constitutive law can be written, incrementally, as

$$d\sigma'_{ij} = D_{ijkl}\left(d\varepsilon_{kl} - d\varepsilon^0_{kl}\right) + \sigma'_{ik}d\omega_{kj} + \sigma'_{jk}d\omega_{ki} \tag{2}$$

where the last two terms account for the Zaremba-Jaumann rotational stress changes (negligible generally in small displacement computation) and D_{ijkl} is a fourth order tangential tensor defined by suitable state variables and the direction of the increment. The incremental strain $d\varepsilon_{ij} = (1/2)(du_{i,j} + du_{j,i})$ and respective rotation $d\omega_{ij} = (1/2)(du_{j,i} - du_{i,j})$ components are defined in the usual way from incremental displacement derivatives and ε^0_{ij} refers to initial strains caused by external actions such as temperature changes, creep, etc.

For a unit control volume, assumed attached to the solid phase and moving with it, the momentum equilibrium equation for the fluid alone can be written as

$$-\kappa p_{,i} - w_i + \kappa \rho_f (b_i - \ddot{u}_i) = \rho_f \left(\dot{w}_i + w_j w_{i,j}\right)/\mu \tag{3}$$

where κ is the isotropic permeability coefficient, according to D'Arcy's seepage law. The equation of flow conservation for the fluid phase can be written in the following form

$$(1/Q)\dot{p} + \alpha \dot{\varepsilon}_{ii} + w_{i,i} + \dot{s}_0 = -(\rho_f/\rho_m)\dot{w}_i \tag{4}$$

where $(1/Q) = \mu/K_f + (\alpha - \mu)/K_s$ and the compression modules of the solid and fluid phases are represented by K_s and K_f, respectively. The rate of volume changes of the fluid is $\dot{s}_0$.

When the acceleration spectrum is composed of low frequencies (i.e., high frequencies contributions can be disregarded), the right hand side of equations (1), (3) and (4) involving the relative acceleration of the fluid are not important and can be omitted with confidence (Zienkiewicz and Shiomi, 1984). The omission of such terms allows for w_i to be eliminated from the governing system of equations, retaining only u_i and p as primary variables (**u**-p formulation). The simplified final system of equations that arises, also considering the dynamic seepage forcing term (i.e., $\kappa \rho_f \ddot{u}_{i,i}$) as negligible, can be written as

$$\sigma_{ij,j} - \rho_m \ddot{u}_i + \rho_m b_i = 0 \tag{5a}$$

$$\alpha \dot{\varepsilon}_{ii} - \kappa p_{,ii} + (1/Q)\dot{p} + a = 0 \tag{5b}$$

where a stands for domain source terms.

Equations (5), accompanied by appropriate initial ($u_i = \bar{u}_{i0}$, $\dot{u}_i = \dot{\bar{u}}_{i0}$ and $p = \bar{p}_0$) and boundary conditions ($u_i = \bar{u}_i$ or $\tau_i = \sigma_{ij} n_j = \bar{\tau}_i$ and $p = \bar{p}$ or $q = p_{,j} n_j = \bar{q}$, where the prescribed values are indicated by over bars and q and τ_i represent fluxes and tractions acting along the boundary whose unit outward normal vector components are represented by n_i), define the model to be solved by the MLPG formulations proposed here.

3 Numerical discretization

Instead of writing the global weak-form for the governing equations described in the previous section, the MLPG method constructs a weak-form over local fictitious sub-domains, such as Ω_s, which is a small region taken for each node inside the global domain. The local sub-domains overlap each other and its geometrical shape

and size can be arbitrary, covering the whole global domain Ω. The local weak-form of the governing equations can be written as

$$\int_{\partial\Omega_s} \varphi_{ik}\sigma_{ij}n_j\,d\Gamma - \int_{\Omega_s} \varphi_{ik,j}\sigma_{ij}\,d\Omega + \int_{\Omega_s} \varphi_{ik}(\rho_m b_i - \rho_m \ddot{u}_i)\,d\Omega + \beta \int_{\Gamma_{su}} \varphi_{ik}(u_i - \bar{u}_i)\,d\Gamma = 0 \quad (6a)$$

$$\int_{\partial\Omega_s} \varphi\,\kappa p_{,i}n_i\,d\Gamma - \int_{\Omega_s} \varphi_{,i}\,\kappa p_{,i}d\Omega + \int_{\Omega_s} \varphi\,(a - (1/Q)\dot{p} - \alpha\dot{\varepsilon}_{ii})\,d\Omega + \beta \int_{\Gamma_{sp}} \varphi\,(p - \bar{p})\,d\Gamma = 0 \quad (6b)$$

where φ and φ_{ik} are test functions and β is a penalty parameter, which is introduced here in order to impose essential prescribed boundary conditions in an integral form. In equations (6), $\partial\Omega_s$ is the boundary of the local sub-domain, which consists of three parts, in general: $\partial\Omega_s = L_s \cup \Gamma_{s1} \cup \Gamma_{s2}$. Here, L_s is the local boundary that is totally inside the global domain, Γ_{s2} is the part of the local boundary which coincides with the global natural boundary, i.e., $\Gamma_{s2} = \partial\Omega_s \cap \Gamma_2$ (where Γ_2 stands for the natural boundary, i.e., $\Gamma_2 \equiv \Gamma_q$ or $\Gamma_2 \equiv \Gamma_\tau$) and, similarly, Γ_{s1} is the part of the local boundary that coincides with the global essential boundary, i.e., $\Gamma_{s1} = \partial\Omega_s \cap \Gamma_1$ (where Γ_1 stands for the essential boundary, i.e., $\Gamma_1 \equiv \Gamma_p$ or $\Gamma_1 \equiv \Gamma_u$).

Taking into account a local approximation to represent the trial functions in terms of nodal unknowns, which are either the nodal values of real field variables or fictitious nodal unknowns at some randomly located nodes (such as in the Moving Least-Square Method), equations (6) can be rewritten in matrix form, following standard MLPG procedures (Soares, 2010a-b). For nonlinear analysis, the matrix systems of equations that arise from equations (6) can be written as

$$\mathbf{M}\ddot{\hat{\mathbf{U}}} + \Im(\hat{\mathbf{U}}) - \mathbf{Q}\hat{\mathbf{P}} = \mathbf{F} \quad (7a)$$

$$\mathbf{C}\dot{\hat{\mathbf{P}}} + \mathbf{H}\hat{\mathbf{P}} + \mathbf{G}\dot{\hat{\mathbf{U}}} = \mathbf{R} \quad (7b)$$

where $\Im$ stands for the internal force vector, computed regarding the nonlinear relations of the model (for the linear elastic particular case, $\Im(\hat{\mathbf{U}}) = \mathbf{K}\hat{\mathbf{U}}$, where $\mathbf{K}$ stands for the stiffness matrix). In equations (7), $\mathbf{M}$ stands for the mass matrix, $\mathbf{C}$

and **H** represent the compressibility and the permeability matrix, respectively, and **Q** and **G** stand for coupling matrices. **F** and **R** are load nodal vectors and $\hat{\mathbf{U}}$ and $\hat{\mathbf{P}}$ stand for unknown nodal values representing the solid matrix displacements and the fluid phase pore-pressures, respectively.

Once the ordinary differential nonlinear matrix equations (7) are established, their coupled solution can be accomplished, taking into account some time-domain iterative technique, such as the Newmark/Newton-Raphson procedure (Soares, 2010b). Considering such a technique, the final coupled system of equations that arises can be given by

$$\begin{bmatrix} (1/(\gamma_2\Delta t^2))\mathbf{M}+\mathbf{K}^T_{(k)} & -\mathbf{Q} \\ (\gamma_1/(\gamma_2\Delta t))\mathbf{G} & (1/(\gamma_3\Delta t))\mathbf{C}+\mathbf{H} \end{bmatrix} \begin{bmatrix} \delta\hat{\mathbf{U}}_{(k+1)} \\ \delta\hat{\mathbf{P}}_{(k+1)} \end{bmatrix} = \begin{bmatrix} \bar{\mathbf{F}}^n_{(k)} \\ \bar{\mathbf{R}}^n_{(k)} \end{bmatrix} \tag{8}$$

where Δt is a selected time-step, superscript n indicates the current step and γ_1, γ_2 and γ_3 are the parameters of the generalized Newmark method. The r.h.s. of equation (8) is defined by

$$\begin{aligned} &\bar{\mathbf{F}}^n_{(k)} = \mathbf{F}^n - \Im(\hat{\mathbf{U}}^n_{(k)}) + \\ &+\mathbf{M}\left(-(1/(\gamma_2\Delta t^2))\, d\hat{\mathbf{U}}^n_{(k)} + (1/(\gamma_2\Delta t))\dot{\hat{\mathbf{U}}}^{n-1} + (1/(2\gamma_2)-1)\ddot{\hat{\mathbf{U}}}^{n-1}\right) + \mathbf{Q}\hat{\mathbf{P}}^n_{(k)} \end{aligned} \tag{9a}$$

$$\begin{aligned} &\bar{\mathbf{R}}^n_{(k)} = \mathbf{R}^n + \mathbf{C}\left(-(1/(\gamma_3\Delta t))d\hat{\mathbf{P}}^n_{(k)} + (1/\gamma_3-1)\dot{\hat{\mathbf{P}}}^{n-1}\right) + \\ &+\mathbf{G}\left(-(\gamma_1/(\gamma_2\Delta t))d\hat{\mathbf{U}}^n_{(k)} + (\gamma_1/\gamma_2-1)\dot{\hat{\mathbf{U}}}^{n-1} + \Delta t(\gamma_1/(2\gamma_2)-1)\ddot{\hat{\mathbf{U}}}^{n-1}\right) - \mathbf{H}\hat{\mathbf{P}}^n_{(k)} \end{aligned} \tag{9b}$$

where $\mathbf{K}^T_{(k)}$ stands for the tangent stiffness matrix. The iterative variations in equations (8) are defined by $\delta\hat{\mathbf{U}}_{(k+1)} = \hat{\mathbf{U}}^n_{(k+1)} - \hat{\mathbf{U}}^n_{(k)}$ and $\delta\hat{\mathbf{P}}_{(k+1)} = \hat{\mathbf{P}}^n_{(k+1)} - \hat{\mathbf{P}}^n_{(k)}$ whereas the iterative increments in equations (9) are defined by $d\hat{\mathbf{U}}^n_{(k)} = \hat{\mathbf{U}}^n_{(k)} - \hat{\mathbf{U}}^{n-1}$ and $d\hat{\mathbf{P}}^n_{(k)} = \hat{\mathbf{P}}^n_{(k)} - \hat{\mathbf{P}}^{n-1}$, where k stands for an iterative step. Equations (8-9), in association with appropriate nonlinear relations, enable the computation of the solid skeleton displacements and interstitial fluid pore-pressures of the model.

For more details regarding dynamic analyses of linear/nonlinear porous media by MLPG techniques, the reader is referred to Soares (2010a-b). In these works, the above equations are deeper discussed taking into MLPG formulations based on Heaviside step functions or Gaussian weight functions as test functions, as well as on the usage of the Moving Least-Square Method to approximate the involved physical quantities, in the local integral equations.

As indicated by equations (8), standard porous media analyses have to solve a coupled system of equations at each iterative step (or time step, in case of linear models). This coupled system is non-symmetric, extremely badly conditioned (the entries of the solid and fluid phase matrices are quite different) and usually large-scale. This is very computationally demanding, especially when nonlinear models are focused.

In the next section, an alternative methodology is introduced in order to analyze each phase of the coupled model independently, through an iterative procedure (uncoupling the system of equations (8)). This methodology renders smaller and better conditioned systems of equations, providing more effective analyses for several applications.

4 Iterative analysis

Considering the iterative framework of the previous section (equations (8-9)), uncoupled analyses of pore-dynamic linear/nonlinear models can be obtained according to the iterative algorithm that follows.

(i) Solid phase analysis:

Firstly in the current iterative step, the solid phase is analyzed, computing the iterative variations of the solid matrix displacements by the solution of the following system of equations

$$[(1/(\gamma_2\Delta t^2))\mathbf{M}+\mathbf{K}^T_{(k)}]\,\delta\hat{\mathbf{U}}_{(k+1)} = \mathbf{F}^n - \Im(\hat{\mathbf{U}}^n_{(k)}) \\ +\mathbf{M}\,(-(1/(\gamma_2\Delta t^2))\,d\hat{\mathbf{U}}^n_{(k)} + (1/(\gamma_2\Delta t))\dot{\hat{\mathbf{U}}}^{n-1} + (1/(2\gamma_2)-1)\ddot{\hat{\mathbf{U}}}^{n-1}) + \mathbf{Q}\hat{\mathbf{P}}^n_{(k)} \quad (10)$$

Once $\delta\hat{\mathbf{U}}_{(k+1)}$ is computed, the solid phase total and incremental displacements are actualized, as indicated below

$$\hat{\mathbf{U}}^n_{(k+1)} = \hat{\mathbf{U}}^n_{(k)} + \delta\hat{\mathbf{U}}_{(k+1)} \quad (11a)$$

$$d\hat{\mathbf{U}}^n_{(k+1)} = \hat{\mathbf{U}}^n_{(k+1)} - \hat{\mathbf{U}}^{n-1} \quad (11b)$$

(ii) Fluid phase analysis:

Considering the solid phase results at the current iterative step, the fluid phase is analyzed. The iterative variations of the interstitial fluid pore-pressures are then

computed by the solution of the following system of equations

$$[(1/(\gamma_3\Delta t))\mathbf{C}+\mathbf{H}]\,\delta\hat{\mathbf{P}}_{(k+1)} = \mathbf{R}^n + \mathbf{C}\,(-(1/(\gamma_3\Delta t))d\hat{\mathbf{P}}^n_{(k)} + (1/\gamma_3 - 1)\dot{\hat{\mathbf{P}}}^{n-1})$$
$$+\mathbf{G}\,(-(\gamma_1/(\gamma_2\Delta t))d\hat{\mathbf{U}}^n_{(k+1)} + (\gamma_1/\gamma_2 - 1)\dot{\hat{\mathbf{U}}}^{n-1} + \Delta t(\gamma_1/(2\gamma_2) - 1)\ddot{\hat{\mathbf{U}}}^{n-1}) - \mathbf{H}\hat{\mathbf{P}}^n_{(k)} \tag{12}$$

and, once $\delta\hat{\mathbf{P}}_{(k+1)}$ is evaluated, the fluid phase variables are actualized as follow

$$\hat{\mathbf{P}}^n_{(k+\lambda)} = \hat{\mathbf{P}}^n_{(k)} + \delta\hat{\mathbf{P}}_{(k+1)} \tag{13a}$$

$$\hat{\mathbf{P}}^n_{(k+1)} = \lambda\,\hat{\mathbf{P}}^n_{(k+\lambda)} + (1-\lambda)\,\hat{\mathbf{P}}^n_{(k)} \tag{13b}$$

$$d\hat{\mathbf{P}}^n_{(k+1)} = \hat{\mathbf{P}}^n_{(k+1)} - \hat{\mathbf{P}}^{n-1} \tag{13c}$$

where λ is a relaxation parameter, introduced here in order to speed up the convergence of the iterative process.

Once the fluid phase variables are computed, the solid phase is analyzed again, reinitiating the iterative cycle. Convergence is achieved once the relative norms of the iterative variations of the solid and fluid phases are lower than a given tolerance.

As one can observe, the present iterative solution is easy to implement and very attractive, since it allows the analysis of reduced and well-conditioned systems of equations. Moreover, nonlinear relations can be carried out within the same iterative steps of the coupled model solution, not introducing a significant additional computational cost for the analysis. The effectiveness of the present iterative algorithm is, however, intimately related to the relaxation parameter selection: an inappropriate selection for λ can considerably increase the number of iterations in the analysis, reducing the advantages of the methodology. In order to obtain a more robust and efficient technique, an expression for an optimal relaxation parameter is presented and discussed in the next subsection. In subsection 5.2, results concerning the introduction of relaxation parameters taking into account different variables of the coupled formulation are presented, further illustrating the effect of relaxation parameters in the current iterative analysis.

4.1 Optimal relaxation parameter

In order to evaluate an optimal relaxation parameter, the following square error functional is here minimized

$$f(\lambda) = ||\hat{\mathbf{P}}^n_{(k+1)} - \hat{\mathbf{P}}^n_{(k)}||^2 \tag{14}$$

Taking into account the relaxation of the pore-pressures for the $(k+1)$ and (k) iterations, equations (15a) and (15b) may be written, regarding relation (13b)

$$\hat{\mathbf{P}}^{n}_{(k+1)} = \lambda\,\hat{\mathbf{P}}^{n}_{(k+\lambda)} + (1-\lambda)\,\hat{\mathbf{P}}^{n}_{(k)} \tag{15a}$$

$$\hat{\mathbf{P}}^{n}_{(k)} = \lambda\,\hat{\mathbf{P}}^{n}_{(k+\lambda-1)} + (1-\lambda)\,\hat{\mathbf{P}}^{n}_{(k-1)} \tag{15b}$$

Substituting equations (15) into equation (14) yields

$$\begin{aligned} f(\lambda) &= ||\,\lambda\mathbf{W}_{(k+\lambda)} + (1-\lambda)\,\mathbf{W}_{(k)}||^2 = \\ &= \lambda^2||\,\mathbf{W}_{(k+\lambda)}||^2 + 2\lambda(1-\lambda)\,(\mathbf{W}_{(k+\lambda)},\mathbf{W}_{(k)}) + (1-\lambda)^2||\,\mathbf{W}_{(k)}||^2 \end{aligned} \tag{16}$$

where the inner product definition is employed (e.g.,$(\mathbf{W},\mathbf{W}) = ||\,\mathbf{W}||^2$) and new variables, as defined in equation (17), are considered.

$$\mathbf{W}_{(k+\ell)} = \hat{\mathbf{P}}^{n}_{(k+\ell)} - \hat{\mathbf{P}}^{n}_{(k+\ell-1)} \tag{17}$$

To find the optimal λ that minimizes the functional $f(\lambda)$, equation (16) is differentiated with respect to λ and the result is set to zero, as described below

$$\lambda||\,\mathbf{W}_{(k+\lambda)}||^2 + (1-2\lambda)\,(\mathbf{W}_{(k+\lambda)},\mathbf{W}_{(k)}) + (\lambda-1)||\,\mathbf{W}_{(k)}||^2 = 0 \tag{18}$$

Re-arranging the terms in equation (18), yields

$$\lambda = (\mathbf{W}_{(k)},\mathbf{W}_{(k)} - \mathbf{W}_{(k+\lambda)})/||\,\mathbf{W}_{(k)} - \mathbf{W}_{(k+\lambda)}||^2 \tag{19}$$

which is an easy to implement expression that provides an optimal value for the relaxation parameter λ, at each iterative step.

It is important to note that the relation $0 < \lambda \leq 1$ must hold. In the present work, the optimal relaxation parameter is evaluated according to equation (19) and if $\lambda \notin (0.01;1.00)$ the previous iterative-step relaxation parameter is adopted. For the first iterative step, $\lambda = 1$ is selected.

5 Numerical Applications

Two numerical applications are considered here, illustrating the discussed methodologies. In the first application, the simulation of a one-dimensional problem is focused, and a soil column is analysed taking into account different material properties. In the second application, a two-dimensional soil strip is considered. The results obtained by the proposed formulation are compared with analytical answers, whenever possible, and with results provided by the Finite Element Method

(FEM). Two MLPG formulations are focused here, namely: (i) MLPG1 – denoting the MLPG formulation that employs Heaviside test functions (Soares, 2010b); (ii) MLPG2 – denoting the MLPG formulation that employs weight functions as test functions (Soares, 2010a). For both formulations the Moving Least-Square Method is adopted to approximate the incognita fields. The time integration parameters are selected according to the trapezoidal rule, i.e.: $\gamma_1 = 0.5$, $\gamma_2 = 0.25$ and $\gamma_3 = 0.5$. Regarding the iterative process, a tolerance error of 10^{-3} is considered for the relative norms of the iterative variations.

5.1 Soil column

In this first example, a soil column is analysed (de Boer *et al.*, 1993; Diebels and Ehlers, 1996; Schanz and Cheng, 2000; Soares, 2008 etc.). A sketch of the model is depicted in Fig.1. The top surface of the column is considered drained and uniformly loaded. The other surfaces of the model are undrained and have null normal displacements prescribed. 561 nodes are employed to spatially discretize the rectangular domain ($H = 10m$).

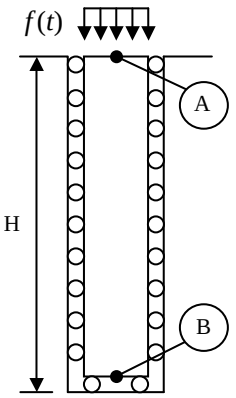

Figure 1: Sketch of the soil column model.

Two kinds of soils and load amplitudes are considered here (the loads have a Heaviside time variation). The properties of the models are specified below:

Model 1 (de Boer *et al.*, 1993; Diebels and Ehlers, 1996; Soares, 2008 etc.) – for the present model, the load amplitude is $3kN/m^2$. The physical properties of the soil are: $\nu = 0.3$ (Poisson); $E = 14515880N/m^2$ (Young Modulus); $\rho_s = 2000kg/m^3$ (mass density – solid phase); $\rho_f = 1000kg/m^3$ (mass density – fluid phase); $\mu = 0.33$ (porosity); $\kappa = 10^{-6}m^4/Ns$ (permeability). The soil is incompressible and the time discretization considered is given by $\Delta t = 10^{-3}s$;

Model 2 (Kim and Kingsbury, 1979; Schanz and Cheng, 2000; Soares, 2008 etc.) – the load amplitude is $1\text{k}N/m^2$. The physical properties of the soil are: $\nu = 0.298$; $E = 254423076.9N/m^2$; $\rho_s = 2700kg/m^3$; $\rho_f = 1000kg/m^3$; $\mu = 0.48$; $\kappa = 3.55 \cdot 10^{-9}m^4/Ns$. The soil is compressible and $K_s = 1.1 \cdot 10^{10}N/m^2$ (compression modulus – solid phase); $K_f = 3.3 \cdot 10^9 N/m^2$ (compression modulus – fluid phase). The time-step is $\Delta t = 10^{-4}s$.

In Fig.2, vertical displacements at point A are depicted, taking into account Model 1. As can be observed, the results obtained by the iterative MLPG formulation are in good agreement with the analytical results provided by de Boer *et al*. (1993) and with the results obtained by the FEM (since the results provided by the MLPG1 and by the MLPG2 are quite similar, just those related to the MLPG1 are depicted in the figure).

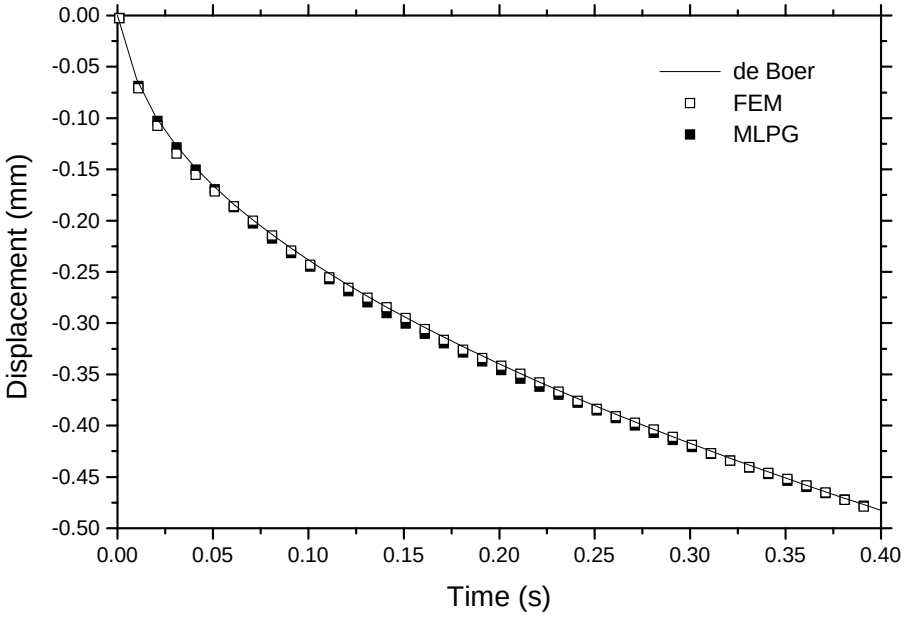

Figure 2: Displacements at point A for the incompressible soil column.

In Fig.3, the evolution of the optimal relaxation parameters, evaluated according to equation (19), is depicted, taking into account MLPG1 and MLPG2. As one can observe in the figure, for both MLPG procedures, the computed relaxation parameters are intricately distributed mostly within the interval (0.75; 1.00). As a matter of fact, optimal relaxation parameters are expected to vary around distinct values during iterative analyses and a constant pre-selection for λ, even when most

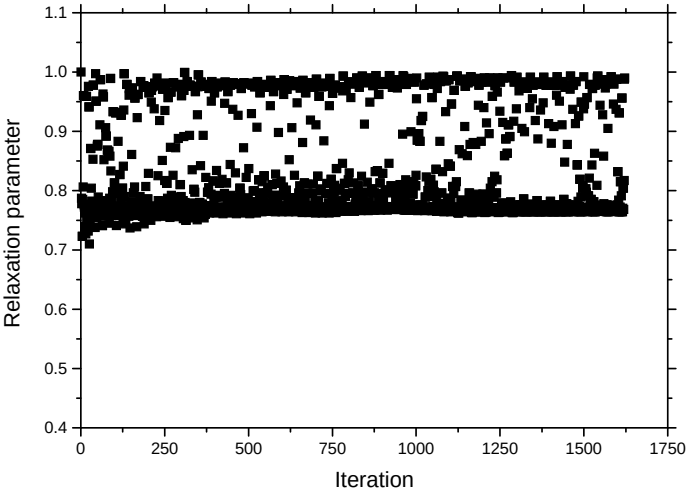

(a)

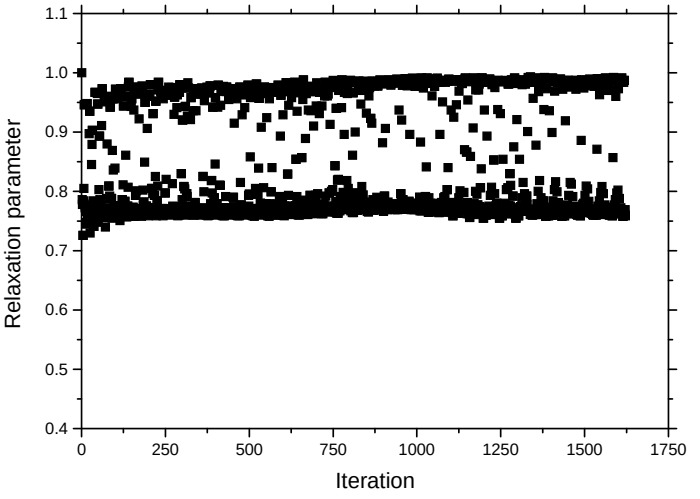

(b)

Figure 3: Optimal relaxation parameters for the incompressible soil column: (a) MLPG1; (b) MLPG2.

appropriated, is unable to account for this dynamic behaviour. It is important to highlight that equation (19) accounts for this dynamic behaviour and that it establishes a correlation between the values of the relaxation parameter and the errors of the iterative procedure, once variable **W** is computed based on iterative residuals (see equation (17)).

Table 1: Average number of iterations per time-step for the MLPG1

Model	Relaxation Parameter	
	Unitary	Optimal
Incompressible soil column	7.105	4.055
Compressible soil column	3.019	2.945
soil strip	25.491	5.917

Table 2: Average number of iterations per time-step for the MLPG2

Model	Relaxation Parameter	
	Unitary	Optimal
Incompressible soil column	7.110	4.055
Compressible soil column	3.016	2.952
soil strip	22.051	5.859

Table 3: Average number of iterations per time-step considering different relaxation procedures (soil strip)

Relaxation Parameter	MLPG1	MLPG2
none	25.491	22.051
λ_p	5.917	5.859
λ_u	8.118	8.282
λ_p & λ_u	8.605	9.105

In Tab.1 and 2, the average number of iterations per time step is presented, considering analyses with optimal relaxation parameters and with a unitary value for λ (which would be the same as an iterative analysis without the introduction of a relaxation parameter). As one can observe, for $\lambda = 1$, an average amount of 7.105 and of 7.110 iterative steps are necessary for convergence, considering the MLPG1 and the MLPG2, respectively. Taking into account optimal relaxation parameters, these values are reduced to 4.055.

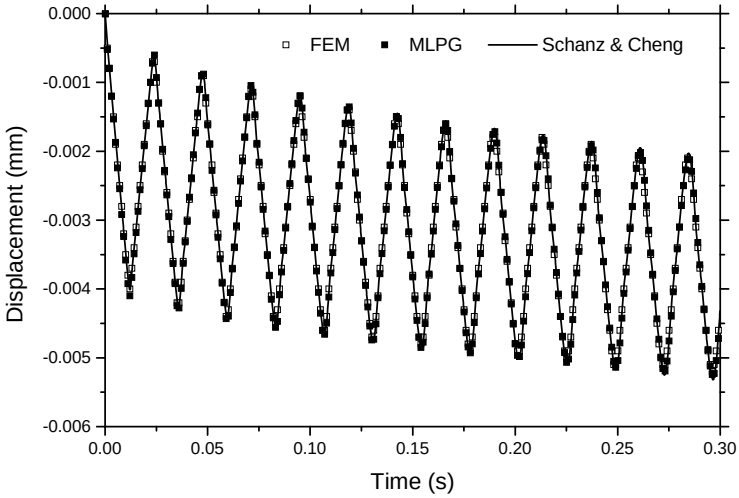

(a)

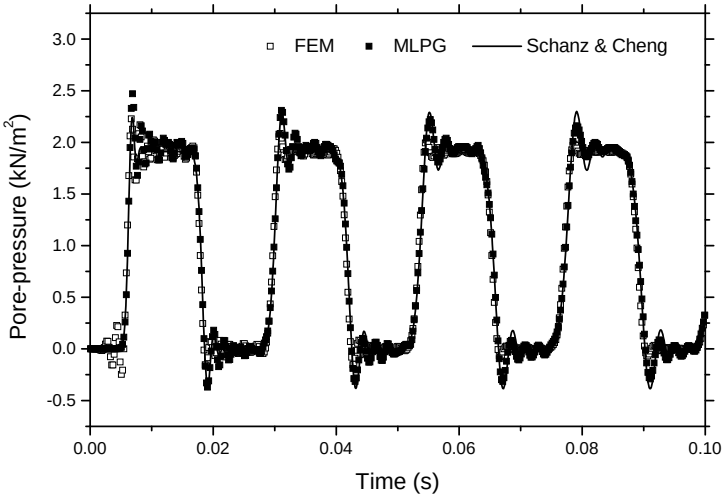

(b)

Figure 4: Compressible soil column: (a) displacements at point A; (b) pore-pressures at point B.

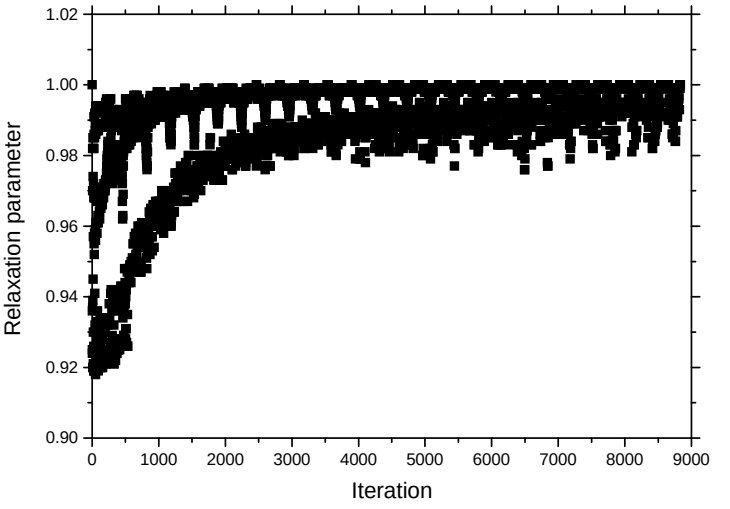

(a)

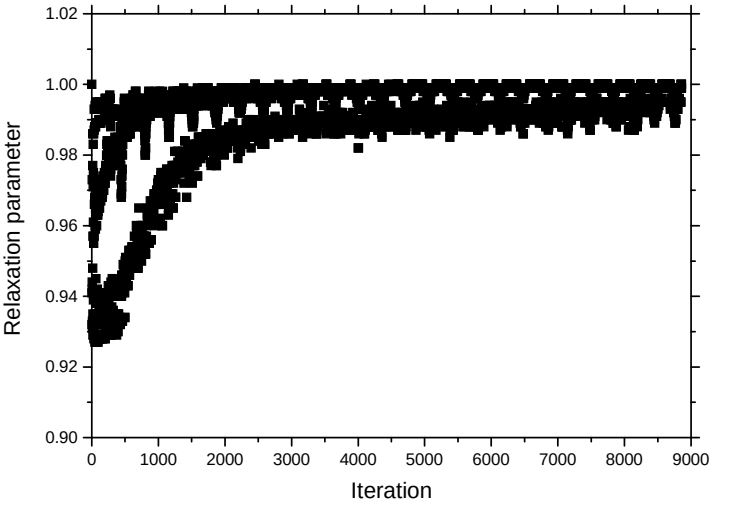

(b)

Figure 5: Optimal relaxation parameters for the compressible soil column: (a) MLPG1; (b) MLPG2.

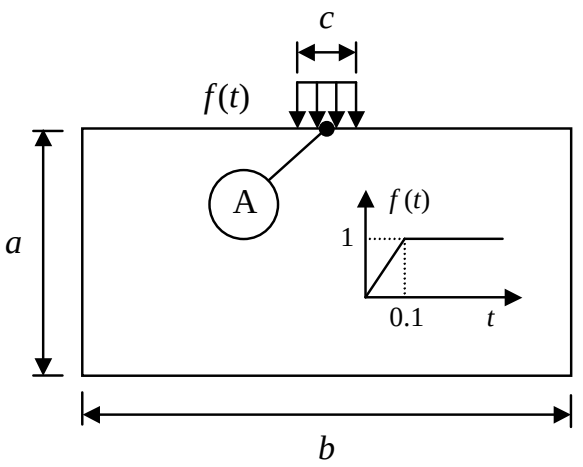

Figure 6: Sketch of the soil strip model.

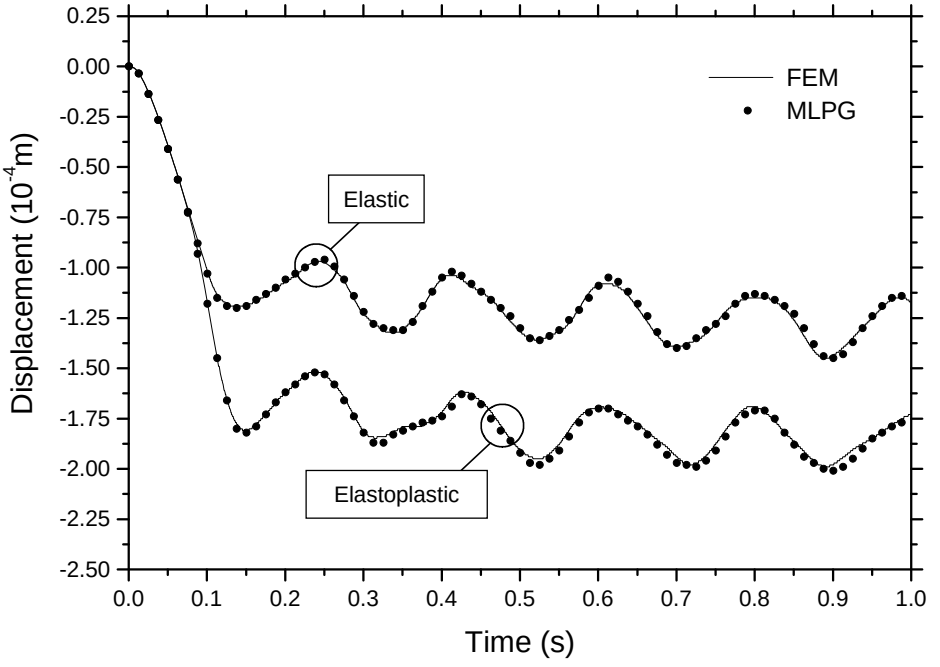

Figure 7: Displacements at point A for the soil strip considering linear and nonlinear behaviour.

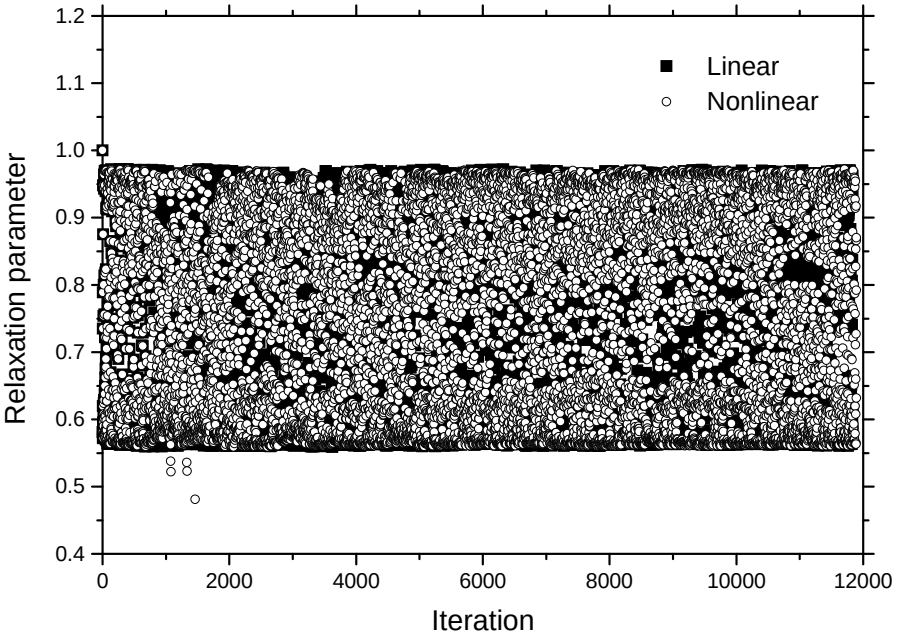

Figure 8: Optimal relaxation parameters for the soil strip considering linear and nonlinear behaviour (MLPG1).

In Fig.4, vertical displacements at point A and pore-pressures at point B are presented, taking into account Model 2. The MLPG results are in good agreement with the results provided by the semi-analytical procedure presented by Schanz and Cheng (2000) and with those provided by the FEM (once again, since MLPG1 and MLPG2 provide similar results, only MLPG1 is depicted).

In Fig.5, the evolution of the optimal relaxation parameters is illustrated, taking into account MLPG1 and MLPG2. As one can observe in Tab.1 and 2, convergence is achieved quite rapidly considering Model 2, even when a relaxation technique is not considered (around 3 iterations per time step are necessary for convergence, in this case). Since this model is already naturally well-suited for the iterative analysis in focus, the optimal relaxation parameter evaluation reflects this fact, and most values computed for λ are around 1, as depicted in Fig.5. These results highlight the assertiveness of the proposed expression (19).

5.2 Soil strip

In this second example, a two-dimensional soil strip is analysed (Li *et al.*, 2003; Soares *et al.*, 2006; Soares, 2008 etc.). A sketch of the model is depicted in Fig.6.

The geometry of the strip is defined by $a = 5\,m$, $b = 10\,m$ and $c = 1\,m$. The symmetry of the model is taken into account and 441 and 121 nodes are employed to spatially discretize the solid and the fluid phase, respectively. An important feature of meshless techniques is that they easily allow the adoption of different phase discretizations (Soares, 2010a), a task which may be quite complex considering some mesh-based formulations, such as the Finite Element Method.

The soil strip is loaded as indicted in Fig.6 (in kN/m^2) and the adopted time-step is $\Delta t = 5 \cdot 10^{-4} s$. The soil is compressible (fluid phase) and $\nu = 0.2$; $E = 10^7 N/m^2$; $\rho_s = 2538.5 kg/m^3$; $\rho_f = 1000 kg/m^3$; $\mu = 0.35$; $\kappa = 10^{-7} m^4/Ns$ and $K_f = 3.3 \cdot 10^9 N/m^2$. A perfectly plastic material obeying the Mohr-Coulomb yield criterion is assumed, where $c = 2 \cdot 10^2 N/m^2$ (cohesion) and $\theta = 10^0$ (internal friction angle).

Vertical displacements at point A (see Fig.6) are depicted in Fig.7, considering linear and nonlinear behaviour (since results related to the MLPG1 and to the MLPG2 are similar, only MLPG1 results are plotted). As can be observed, the results provided by the proposed formulation are in good agreement with those provided by the FEM. In Fig.8, the evolution of the optimal relaxation parameters is illustrated (MLPG1), taking into account linear and nonlinear behaviour. For this application, the computed relaxation parameters are intricately distributed mostly within the interval (0.55; 1.00). As one can observe in Tab.1 and 2, for the present application, the introduction of optimal relaxation parameters expressively reduces the number of iterations in the analysis. For the linear case, the average number of iterations per time-step is reduced from 25.491 to 5.917, considering the MLPG1, and from 22.051 to 5.859, considering the MLPG2. It is also important to note that nonlinear analyses can be carried out without introducing a significant increase in the computational costs of the iterative procedure: considering the MLPG1, the average number of iterations per time-step in the linear case was 5.917 whereas for the nonlinear case it was 5.947.

In the relaxation procedure described in section 4, the relaxation parameters are introduced in the actualization of the pore-pressure variables (equations (13)); however, several other techniques are possible. As for instance, the relaxation parameters could be introduced in the actualization of the displacement variables (equations (11)), or in the actualization of both pore-pressure and displacement variables. In Tab.3, the average number of iterations per time step is presented considering these different relaxation procedures. The nomenclature adopted in Tab.3 is defined as follows: (i) for the λ_p case, optimal relaxation parameters are considered just for the actualization of the pore-pressure variables (as described in section 4); (ii) for the λ_u case, optimal relaxation parameters are considered just for the actualization of the displacement variables; and (iii) for the λ_p & λ_u case, optimal relaxation parameters are considered for the actualization of both pore-pressure and

displacement variables. For all cases, computation of optimal values is carried out analogously to what is presented in subsection 4.1. As one can observe in Tab.3, introduction of relaxation parameters just in the actualization of the pore-pressure variables provides more efficient analyses. Similar results are obtained considering other applications, thus, this relaxation procedure was selected to be presented in section 4.

6 Conclusions

An iterative procedure was presented to analyse pore-dynamic models discretized by time-domain MLPG formulations. The introduction of optimal relaxation parameters was considered, taking into account a low computational cost and easy to implement equation, expressively improving the efficiency of the methodology. As described in the discussed numerical examples, the proposed formulation allows convergence to be achieved considering just few iterative steps. Two MLPG formulations were focused and similar results were obtained for them (and they are expected for other similar MLPG approaches). Nonlinear analyses were also considered, indicating that the iterative solution of the coupled system of equations can also handle the analysis of the nonlinear relations without increasing the computational effort of the procedure.

The proposed iterative methodology exhibits several advantages, such as: (i) each phase of the model can be analysed separately, leading to smaller and better-conditioned systems of equations; (ii) different solvers and modelling numerical procedures, such as completely different spatial and temporal discretization techniques, can be easily considered for each phase of the model, rendering more flexible and accurate analyses; (iii) only interface routines are required when one wishes to use existing codes to build coupling algorithms; (iv) nonlinear analyses can be easily carried out within the framework of the iterative solution of the coupled equations; etc. Another major advantage of the present iterative formulation (to be explored in future works) regards the facility to introduce adaptive techniques (for each phase of the model independently) within the framework of the iterative solution, a procedure which is very appropriate taking into account truly meshless formulations, such as the MLPG.

Acknowledgement: The financial support by CNPq (*Conselho Nacional de Desenvolvimento Científico e Tecnológico*) and FAPEMIG (*Fundação de Amparo à Pesquisa do Estado de Minas Gerais*) is greatly acknowledged.

References

Atluri, S.N.; Shen, S.P. (2002): The meshless local Petrov-Galerkin (MLPG) method: A simple & less costly alternative to the finite element and boundary element methods, *CMES: Computer Modeling in Engineering & Sciences* vol.3, pp. 11-51.

Atluri, S.N.; Zhu, T. (1998): A New Meshless Local Petrov-Galerkin (MLPG) Approach in Computational Mechanics, *Computational Mechanics* vol.22, pp. 117-127.

Belytschko, T., Lu, Y., Gu, L. (1994): Element free Galerkin methods, *International Journal for Numerical Methods in Engineering* vol.37, pp. 229-256.

Bergamaschi, L. (2009): An Efficient Parallel MLPG Method for Poroelastic Models, *CMES: Computer Modeling in Engineering & Sciences* vol.29, pp. 191-215.

Biot, M.A. (1941): General theory of three-dimensional consolidation, *Journal of Applied Physics* vol.12, pp. 155–164.

Biot, M.A. (1956): The theory of propagation of elastic waves in a fluid-saturated porous solid. I. Low frequency range, *Journal of the Acoustical Society of America* vol.28, pp. 167–178.

Biot, M.A. (1956): The theory of propagation of elastic waves in a fluid-saturated porous solid. II. Higher frequency range, *Journal of the Acoustical Society of America* vol.28, pp. 179–191.

Biot, M.A. (1962): Mechanics of deformation and acoustic propagation in porous media, *Journal of Applied Physics* vol.33, pp. 1482–1498.

Cavalcanti, M.C., Telles, J.C.F. (2003): Biot's consolidation theory — application of BEM with time independent fundamental solutions for poro-elastic saturated media, *Engineering Analysis with Boundary Elements* vol. 27, pp. 45–57.

de Boer, R. (1998): *Theory of porous media – highlights in the historical development and current state*, Springer, Berlin.

de Boer, R., Ehlers, W., Liu, Z. (1993): One-dimensional transient wave propagation in fluid saturated incompressible porous media, *Archive of Applied Mechanics* vol.63, pp. 59-72.

Diebels, S., Ehlers, W. (1996): Dynamic analysis of a fully saturated porous medium accounting for geometrical and material non-linearities. *International Journal for Numerical Methods in Engineering* vol.49, pp. 833-848.

Ehlers, W., Bluhm J. (eds) (1998): *Porous media – theory, experiments and numerical applications*, Springer, Berlin.

Ferronato, M., Mazzia, A., Pini, G., Gambolati, G. (2007): A meshless method for axi-symmetric poroelastic simulations: Numerical study, *International Journal for Numerical Methods in Engineering* vol.70, pp. 1346-1365.

Kim, Y. K., Kingsbury, H. B. (1979): Dynamic characterization of poroelastic materials. *Experimental Mechanics* vol.19, pp. 252-258.

Lewis, R.W., Schrefler, B.A. (1998): *The finite element method in the static and dynamic deformation and consolidation of porous media* (2^{nd} ed), John Wiley & Sons, Chichester.

Li, X., Han, X., Pastor, M. (2003): An iterative stabilized fractional step algorithm for finite element analysis in saturated soil dynamics, *Computational Methods in Applied Mechanics and Engineering* vol.192, pp. 3845-3859.

Markert, B., Heider, Y., Ehlers, W. (2010): Comparison of monolithic and splitting solution schemes for dynamic porous media problems, *International Journal for Numerical Methods in Engineering* vol.82, pp. 341-1383.

Mikhailov, S.E. (2002): Localized boundary-domain integral formulations for problems with variable coefficients, *Engineering Analysis with Boundary Elements* vol.26, pp. 681-690.

Schanz, M., Cheng, A.H.D. (2000): Transient wave propagation in a one-dimensional poroelastic column, *Acta Mechanica* vol.145, pp. 1-18.

Sladek, J.; Sladek, V.; Zhang, C.Z. (2003): Application of meshless local Petrov-Galerkin (MLPG) method to elastodynamic problems in continuously nonhomogeneous solids, *CMES: Computer Modeling in Engineering & Sciences* vol.4, pp. 637-647.

Sladek, J.; Sladek, V.; Zhang, C.H. (2008): Computation of stresses in nonhomogeneous elastic solids by local integral equation method: a comparative study, *Computational Mechanics* vol.41, pp. 827-845.

Soares Jr., D. (2008): A time-domain FEM approach based on implicit Green's functions for the dynamic analysis of porous media, *Computational Methods in Applied Mechanics and Engineering* vol.197, pp. 4645–4652.

Soares Jr., D. (2010a): Dynamic Analysis of Porous Media Considering Unequal Phase Discretization by Meshless Local Petrov-Galerkin Formulations, *CMES: Computer Modeling in Engineering & Sciences* vol.61, pp. 177–200.

Soares Jr., D. (2010b): A Time-Domain Meshless Local Petrov-Galerkin Formulation for the Dynamic Analysis of Nonlinear Porous Media, *CMES: Computer Modeling in Engineering & Sciences* vol.66, pp. 227-248.

Soares Jr., D., Telles, J.C.F., Mansur, W.J. (2006): A time-domain boundary element formulation for the dynamic analysis of non-linear porous media, *Engineering*

Analysis with Boundary Elements vol.30, pp. 363-370.

Wang, J.G., Xie, H., Leung, C.F. (2009): A local boundary integral-based meshless method for Biot's consolidation problem, *Engineering Analysis with Boundary Elements* vol.33, pp. 35-42.

Zienkiewicz, O.C., Chan, A.H.C., Pastor, M., Paul, D.K., Shiomi, T (1990): Static and dynamic behavior of soils: a rational approach to quantitative solutions. I. Fully saturated problems, *Proceedings of the Royal Society of London* vol.429, pp. 285-309.

Zienkiewicz, O.C., Chan, A.H.C., Pastor, M., Schrefler, B.A., Shiomi, T. (1999): *Computational geomechanics with special reference to earthquake engineering*, John Wiley & Sons, Chichester.

Zienkiewicz, O.C., Shiomi, T. (1984): Dynamic behavior of saturated porous media: the generalized Biot formulation and its numerical solution, *International Journal for Numerical and Analytical Methods in Geomechanics* vol.8, pp. 71-96.